BIOCHEMISTRY
including biophysical chemistry & molecular biology

Article

pubs.acs.org/biochemistry

Scavenger Receptor Class B Type I Regulates Plasma Apolipoprotein E Levels and Dietary Lipid Deposition to the Liver

Eleni A. Karavia,[†] Nikolaos I. Papachristou,[‡] George C. Sakellaropoulos,[§] Eva Xepapadaki,[†] Eleni Papamichail,[†] Peristera-Ioanna Petropoulou,[†] Eugenia P. Papakosta,[†] Caterina Constantinou,[†] Ioannis Habeos,[∥] Dionysios J. Papachristou,[‡] and Kyriakos E. Kypreos*[,†]

[†]Pharmacology Department, [‡]Anatomy Histology and Embryology Department, [§]Medical Physics Department, and [∥]Endocrinology Department, University of Patras Medical School, Rio Achaias, TK 26500, Greece

Supporting Information

ABSTRACT: Scavenger receptor class B type I (SR-BI) is primarily responsible for the selective uptake of cholesteryl esters (CE) of high-density lipoprotein (HDL) by the liver and other tissues. In the present study, we show that SR-BI-deficient (*scarb1*$^{-/-}$) mice are resistant to diet-induced obesity, hepatic lipid deposition, and glucose intolerance after 24 weeks of being fed a western-type diet. No differences in energy expenditure or mitochondrial function could account for the observed phenotype. Kinetic and gene expression analyses suggested reduced *de novo* fatty acid synthesis in *scarb1*$^{-/-}$ mice. Furthermore, adenosine monophosphate-activated protein kinase (AMPK)-stimulated hepatic FFA catabolism was reduced in these mice, leaving direct dietary lipid uptake from plasma as the major modulator of hepatic lipid content. Analysis of the apolipoprotein composition of plasma lipoproteins revealed a significant accumulation of apolipoprotein E (ApoE)-containing HDL and TG-rich lipoproteins in *scarb1*$^{-/-}$ mice that correlated with reduced plasma LpL activity. Our data suggest that *scarb1*$^{-/-}$ mice fed a western-type diet for 24 weeks accumulate CE- and ApoE-rich HDL of abnormal density and size. The elevated HDL-ApoE levels inhibit plasma LpL activity, blocking the clearance of triglyceride-rich lipoproteins and preventing the shuttling of dietary lipids to the liver.

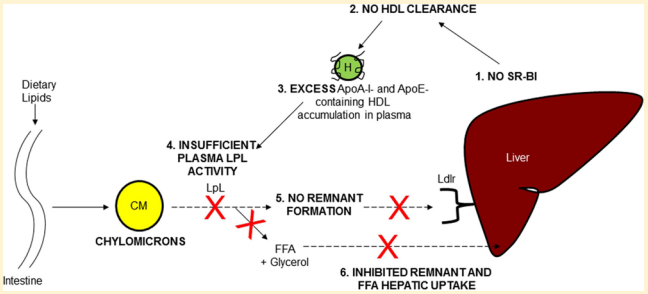

Scavenger receptor class B member I (SR-BI) is an 82 kDa cell-surface glycoprotein that belongs to the CD36 superfamily along with mammalian scavenger receptor CD36 and lysosomal membrane protein 2.[1] SR-BI is widely expressed, including tissues such as adrenal and gonad and cells such as macrophages and endothelial cells (primarily in the liver),[2,3] where it mediates the binding to very-low-density lipoproteins (VLDL), intermediate-density lipoproteins (LDL), and high-density lipoproteins (HDL).[2,4] The main function of SR-BI is the selective uptake of cholesteryl esters (CE) from HDL, thus reducing its size.[5−8] Additional studies suggest that SR-BI in macrophages binds oxidized LDL (oxLDL), forming foam cells,[9] although some studies support that this binding is not as efficient as the binding of oxLDL to CD36.[10] In terms of the effects of SR-BI on mouse physiology, overexpression of SR-BI in the liver of SR-BI-deficient (*scarb1*$^{-/-}$) animals by adenovirus-mediated gene transfer results in decreased plasma HDL cholesterol (HDL-C) and apolipoprotein A-I (ApoA-I) levels,[11] whereas liver-specific SR-BI transgenic mice (SR-BI-Tg) display reduced plasma apolipoprotein A-II (ApoA-II) and B (ApoB) levels.[12] On the other hand, ubiquitous deletion of *scarb1* correlates with high levels of total plasma cholesterol and increased cholesterol in HDL fractions.[13] In agreement with the important role of SR-BI in reverse cholesterol transport (RCT), *scarb1*$^{-/-}$ mice challenged with high-fat diet for 20 weeks develop aortic lesions, confirming the antiatherogenic function of SR-BI.[14]

Nonalcoholic fatty liver disease (NAFLD) is a chronic disease characterized by fat accumulation in hepatocytes of people who consume little or no alcohol. It has been proposed to be the hepatic component of metabolic syndrome[15,16] since recent data indicate that, in patients with metabolic syndrome, hyperinsulinemia induces a series of hepatic disturbances, such as increased hepatic *de novo* lipogenesis, impaired inhibition of adipose tissue lipolysis, and increased efflux of free fatty acids from adipose tissue to the liver, setting the stage for the development of NAFLD.[17] NAFLD shows increased prevalence worldwide that correlates closely with the obesity epidemic (70−80% of obese patients have the disease).[18] Epidemiological data indicate that 20% of the general population suffer from NAFLD worldwide, which is further increased to 70% in patients with type 2 diabetes mellitus.[19]

Recent data suggested that the coexistence of low levels and/or dysfunctional HDL with NAFLD in metabolic syndrome may not be a mere coincidence; rather, it underpins a strong causative relationship between these two conditions.[20,21] In the

Received: June 23, 2015
Revised: August 27, 2015
Published: August 27, 2015

DOI: 10.1021/acs.biochem.5b00700
Biochemistry 2015, 54, 5605−5616

present study, we sought to investigate the biochemical mechanisms mediating the effects of SR-BI on plasma ApoE levels and dietary lipid deposition to the liver. Our data indicate that deficiency in SR-BI results in diet-induced accumulation of apolipoprotein E (ApoE)-rich lipoproteins and a reduction of LpL activity in plasma that ultimately attenuates clearance of all TG-rich lipoproteins and the shuttling of dietary lipids from the intestine to the liver.

MATERIALS AND METHODS

Animals. *Scarb1*$^{+/-}$ mice[13] were back-crossed in our animal facility for nine generations to C57BL/6 mice to ensure that their genetic background is similar to that of the control group. Breeding heterozygote *scarb1*$^{+/-}$ mice gave rise to *scarb1*$^{-/-}$ mice that were identified by PCR genotyping according to Jackson Laboratories' protocol (Figure S1, Supporting Information). Wild-type C57BL/6 littermates were used as controls. Unless otherwise indicated, for each study, female mice 10−12 weeks old were caged individually (one mouse per cage) and were allowed unrestricted access to food and water under a 12 h light/dark cycle (7.00 am to 6.59 pm light). Groups of mice were formed in which average cholesterol, triglycerides (TG), and glucose levels and starting body weights were ensured to be similar. Mice were fed the standard western-type diet (Mucedola SRL, Milano, Italy)[20,21] for the indicated periods. At the end of each experiment, mice were sacrificed, and plasma and tissue samples were collected for histological and biochemical analyses. All animal studies were conducted according to EU guidelines for the Protection and Welfare of Animals. The estimated sample size was determined based on the desired power of statistical analysis, using an online statistical tool (http://www.stat.ubc.ca/~rollin/stats/ssize/n2.html). The work was authorized by the Laboratory Animal Center committee of The University of Patras Medical School and the Veterinary Authority of the Prefecture of Western Greece.

Mouse Genotyping. Mouse genotyping was performed by PCR analysis of genomic DNA isolated from tail biopsies according to Jackson Laboratories' protocol. PCR products were analyzed on an 1.5% agarose−TAE gel, and the 100 bp DNA ladder (cat. no. N3231L, New England Biolabs, Ipswich, MA, USA) was used to confirm the size of DNA bands (Figure S1, Supporting Information).

Determination of Body Weight and Daily Food Consumption. At the indicated time-points during the course of the experiments, six mice in each group were briefly anesthetized using isofluorane, and their body weight was determined by a Mettler precision microscale. At the same time points, food intake was assessed during a 7 day period to ensure reliable measurements, as described previously.[22,23] Food intake was then expressed as the average of all measurements for each group during the entire duration of the experiment and is reported as the mean ± standard error of the mean.

Determination of Postprandial Triglyceride Kinetics Following Oral Administration of Olive Oil. Groups of six *scarb1*$^{-/-}$ and C57BL/6 mice were used. Determination of the postprandial TG kinetics was performed by oral (gavage) administration of 300 μL of extra virgin olive oil, as described previously.[24] Values are expressed in mg/dL ± standard error of the mean.

Rate of Hepatic VLDL-Triglyceride Secretion. The rate of hepatic VLDL-triglyceride (VLDL-TG) secretion was measured as described previously.[21,25,26]

Fasting Glucose Determination, GTT, and IST. Fasting plasma levels were determined after a 16 h fasting period (starting at 7.00 pm) using a Bayer Contour glucometer (Bayer, Germany). Glucose tolerance test (GTT) and insulin sensitivity test (IST) were performed as described previously[23] using doses of 2 g of dextrose per kilogram of body weight and 1 U of humulin per kilogram of body weight, respectively. Groups of six *scarb1*$^{-/-}$ and C57BL/6 mice were studied.

Insulin Quantification by ELISA. Plasma insulin levels during GTT were evaluated by ELISA (rat/mouse insulin ELISA kit, cat. no. EZRMI-13K, Merck, USA) according to the manufacturer's instructions. Groups of six *scarb1*$^{-/-}$ and C57BL/6 mice were studied.

Indirect Calorimetry Studies. Indirect calorimetry studies were performed using the Phenomaster small animal colorimetry system (TSE Systems, Germany), as described previously.[20,27] Six *scarb1*$^{-/-}$ and seven C57BL/6 mice were analyzed per group.

Plasma Lipid Determination. Following a 16 h fasting period (starting at 7.00 pm), plasma samples were isolated from the experimental mice via tail vein. Total plasma cholesterol and plasma TG levels were measured as described previously.[28] Groups of six *scarb1*$^{-/-}$ and C57BL/6 mice were studied.

Fractionation of Plasma Lipoproteins by Density Gradient Ultracentrifugation. For the determination of total plasma cholesterol, plasma TG, free cholesterol, and CE in various plasma lipoproteins, 0.5 mL of pools of plasma from six *scarb1*$^{-/-}$ and six C57BL/6 mice was fractionated by density gradient ultracentrifugation (UCF), as described previously.[28]

Measurement of Total Hepatic TG Content. Total hepatic TG determination was performed as described previously.[24] Groups of six *scarb1*$^{-/-}$ and C57BL/6 mice were studied. Results are expressed as milligrams of TG per gram of tissue ± standard error of the mean.

Histological Analysis of Tissue Samples. Conventional hematoxylin−eosin (H&E) and reticulin histological stainings of hepatic sections were performed as described previously.[20,21] Groups of six *scarb1*$^{-/-}$ and C57BL/6 mice were studied.

Isolation of Pure Mitochondria. Mitochondria from brown adipose tissue (BAT) were isolated from three *scarb1*$^{-/-}$ and three C57BL/6 mice as described previously.[29] The protein concentration of each mitochondrial sample was determined using the detergent-compatible protein assay kit (Bio-Rad Laboratories, cat. no. 500-0006).

Western Blot Analysis. Western blot analysis of ApoA-I and ApoE in UCF lipoprotein fractions was performed as described previously[28] using a goat anti-human ApoA-I antibody (Biodesign International, cat. no. K45252G) and goat anti-human ApoE antibody (Biodesign International, cat. no. K74190G), respectively, as the primary and a rabbit anti-goat antibody (Santa Cruz, cat. no. sc-2768) as the secondary. For western blot analysis of total adenosine monophosphate-activated protein kinase (AMPK) levels in liver lysates from *scarb1*$^{-/-}$ and C57BL/6 mice, a rabbit anti-mouse AMPK antibody was used (Cell Signaling, cat. no. 2532), whereas AMPK phosphorylation at Thr172 was estimated using a rabbit anti-mouse P(Thr172) antibody (Cell Signaling, cat. no. 2535). Western blotting analysis of murine cytochrome c (CytC), uncoupling protein 1 (Ucp1), and cytochrome c oxidase subunit 4 (COx4) was performed using primary rabbit anti-mouse IgG antibodies (cat. no. 4272, Cell Signaling, Danvers, MA; cat. no. GTX10983, Acris, Herford, Germany; cat. no.

DOI: 10.1021/acs.biochem.5b00700
Biochemistry 2015, 54, 5605−5616

Table 1. Statistical Results Following Two-Way Repeated Measures ANOVA of Our Results

	time			genotype			time[a]−genotype interaction		
figure	*F*	*DF*	*p*	*F*	*DF*	*p*	*F*	*DF*	*p*
2A[a]	33.37	2.015	<0.001[b]	0.9	1	0.371	3.26	2.015	0.064
2B	48.01	4	<0.001[b]	28.92	1	0.006[c]	16.01	4	<0.001[d]
2C[a]	25.01	1.536	<0.001[b]	10.59	1	0.012[c]	1.41	1.536	0.273
2D	10.87	4	<0.001[b]	0.78	1	0.444	0.90	4	0.497
2E	4.23	4	0.023[b]	11.37	1	0.043[c]	3.59	4	0.038[d]
4A	3.77	2	0.070	54.59	1	0.002[c]	2.92	2	0.112
4B	168.40	2	<0.001[b]	35.72	1	0.001[c]	29.71	2	<0.001[d]
4C	4.51	6	0.002[b]	16.78	1	0.009[c]	0.90	6	0.506

[a]Mauchly's sphericity test was significant at the 0.05 level; therefore, the Greenhouse−Geisser degrees of freedom adjustment was performed. [b]The curves differ significantly from the horizontal. [c]The curves of the two genotypes are significantly different. [d]The observed difference between genotypes is not identical at all time points.

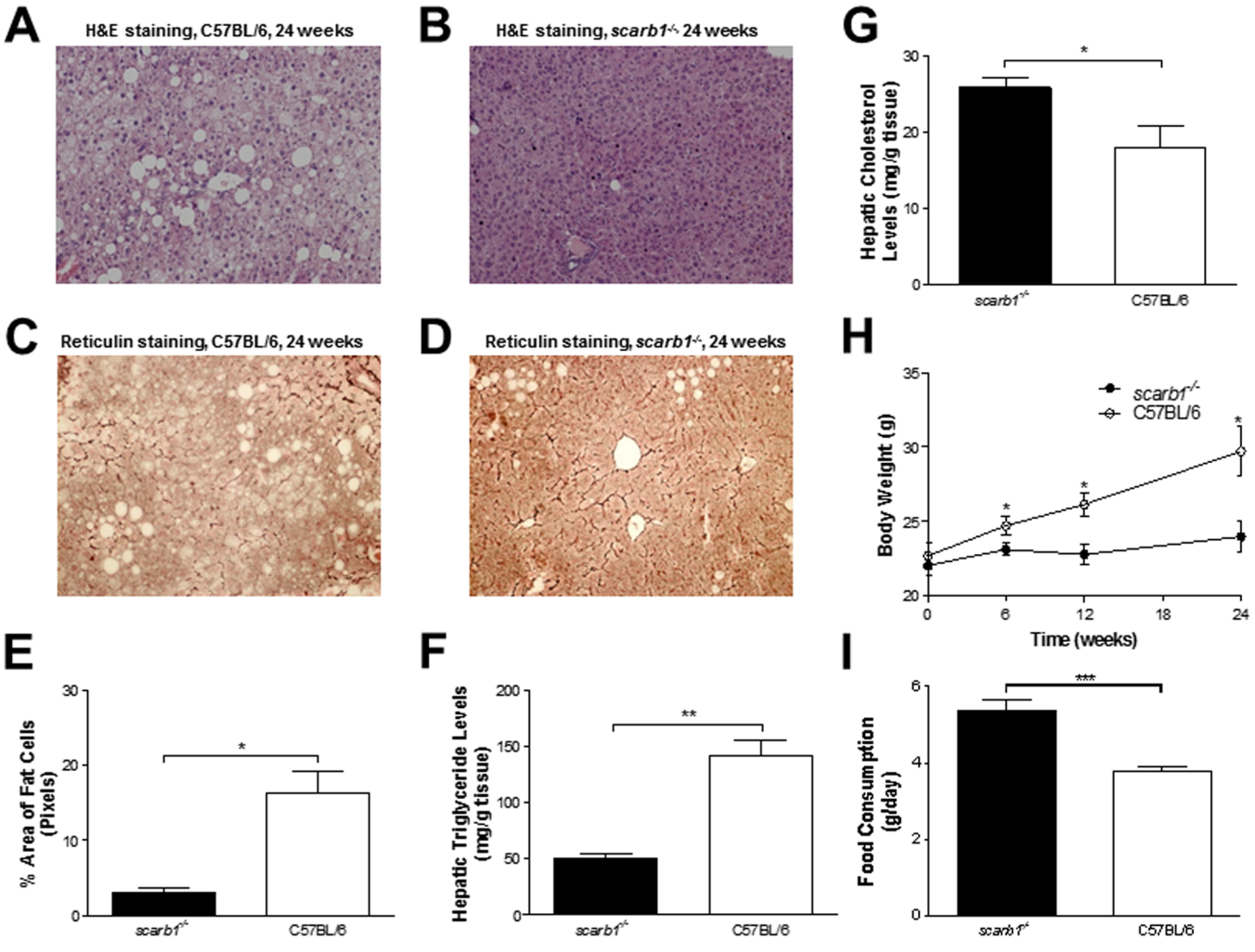

Figure 1. Histological analyses of liver sections from C57BL/5 and *scarb1*$^{-/-}$ mice fed a western-type diet for 24 weeks. (A, B) Representative pictures of H&E-stained hepatic sections from C57BL/6 (A) or *scarb1*$^{-/-}$ (B) mice. (C, D) Representative pictures of extracellular reticulin-stained hepatic sections from C57BL/6 (C) or *scarb1*$^{-/-}$ (D) mice. All pictures in panels A−D were taken under an original magnification of 20×. (E) Average surface area of lipid-loaded cells in the livers of *scarb1*$^{-/-}$ (■) and C57BL/6 (□) mice. (F) Biochemical determination of hepatic TG content of *scarb1*$^{-/-}$ (■) and C57BL/6 (□) mice. (G) Biochemical determination of hepatic cholesterol content of *scarb1*$^{-/-}$ (■) and C57BL/6 (□) mice. (H) Body weight changes as a function of time in *scarb1*$^{-/-}$ (●) and C57BL/6 (○) mice during the course of the experiment. (I) Average food consumption of *scarb1*$^{-/-}$ (●) and C57BL/6 (○) mice during the course of the experiment.

Ab165056, AbCam, Cambridge, UK, respectively) as described previously.[27]

Real-Time PCR Analysis of Gene Expression. Real-Time PCR for *apoe*, fatty acid synthase (*fasn*), peroxisome proliferator-activated receptor gamma (*ppargamma*), diacylglycerol acyltransferase isoform 1 (*dgat1*), low-density lipoprotein receptor (*ldlr*), low-density lipoprotein receptor-related protein 1(lrp1), and 40S ribosomal protein S18 (rps18) (a house-

DOI: 10.1021/acs.biochem.5b00700
Biochemistry 2015, 54, 5605−5616

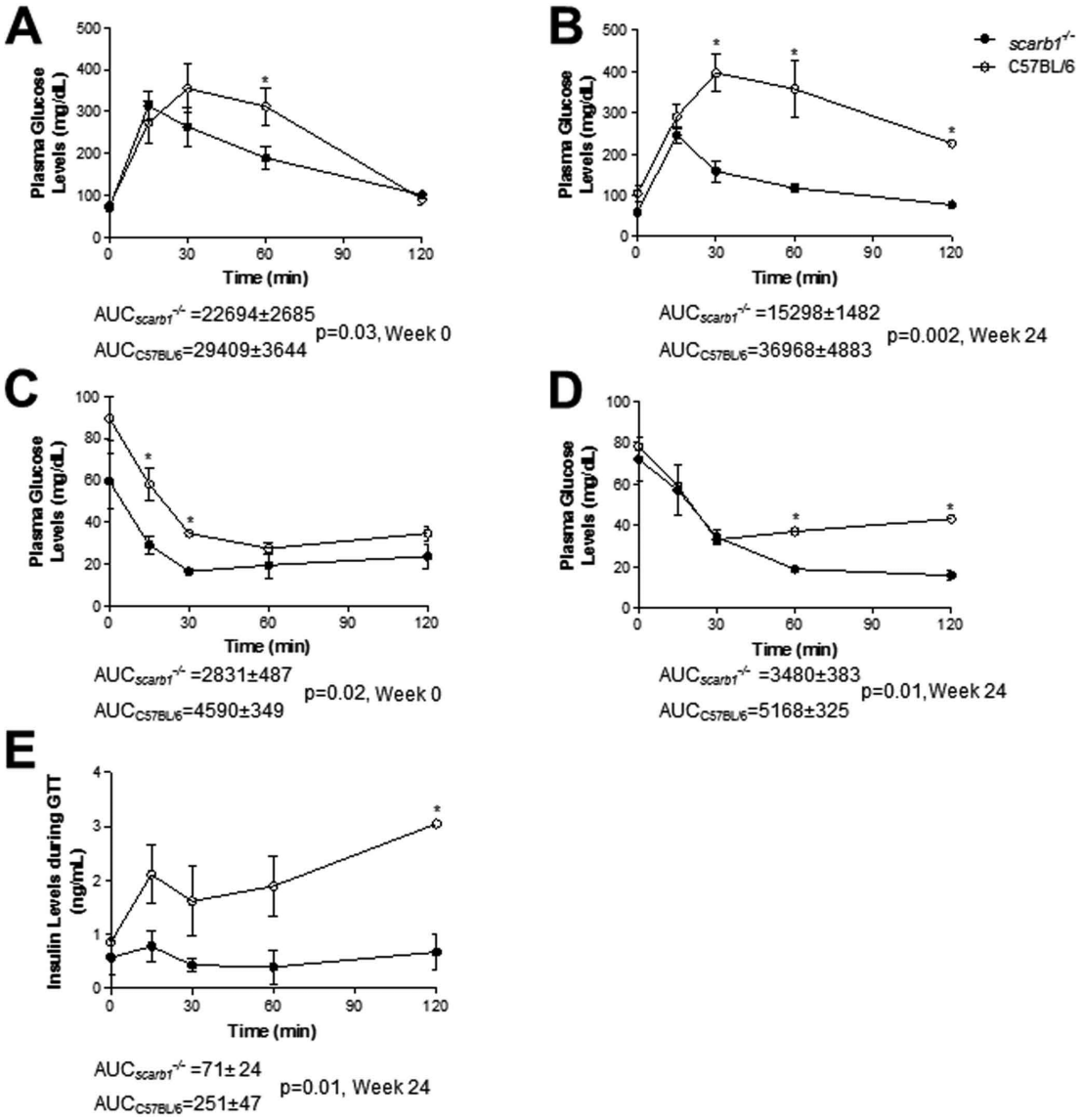

Figure 2. Effects of SR-BI deficiency on glucose tolerance (A, B), insulin sensitivity (C, D), and plasma insulin levels during GTT (E) in *scarb1*$^{-/-}$ and C57BL/5 mice fed a western-type diet for 24 weeks. Data in all panels are reported as the mean ± standard error of the mean. * indicates $p < 0.05$. In panels A–D, AUG is expressed in mg/dL/min, and in panel E, in ng/mL/min.

keeping gene) was performed as described previously.[27] The primers used for *mc2r* analysis were as follows: forward: 5′-TCT TAA GCC TCG TGG CAG TT-3′, reverse: 5′-GCT ATG GTA TTG CAG GGC AT-3′. The primers used for *pparalpha* analysis were as follows: forward: 5′-TAT TCG GCT GAA GCT GGT GTA C-3′, reverse: 5′-CTG GCA TTT GTT CCG GTT CT-3′. The primers used for *pgc1a* analysis were as follows: forward: 5′-GGA TTG AAG TGG TGT AGC GAC-3′, reverse: 5′-GCT CAT TGT TGT ACT GGT TGG A-3′. Groups of six *scarb1*$^{-/-}$ and C57BL/6 mice were studied.

Ectopic Expression of LpL by Adenovirus-Mediated Gene Transfer in SR-BI-Deficient Mice. Two groups of five *scarb1*$^{-/-}$ mice each were formed and fed a western-type diet for 10 weeks. At the end of this period, one group received intravenously, via the tail vein, 5×10^8 pfu of a human LpL-expressing adenovirus (AdLpL),[30,31] and the second group received 5×10^8 pfu of a control adenovirus, AdGFP. Three days following infection, blood samples were collected and plasma was isolated for triglyceride determination. To verify the activity of LpL *in vivo*, ApoE$^{-/-}$ mice infected with 2×10^9 pfu of ApoE2-expressing adenovirus (AdGFP-E2) were coinfected with either 5×10^8 pfu of Ad-LpL or 5×10^8 pfu of the empty AdGFP adenovirus. Three days following infection, plasma triglyceride levels were determined as described previously.[32] The Ad-LpL adenovirus was a kind gift of Dr. Silvia Santamarina-Fojo,[30,31] and the AdGFP and AdGFP-E2 adenoviruses have been described previously.[32]

Statistical Analysis. Data are reported as the mean ± estimated standard error of the mean. * indicates $p < 0.05$, ** indicates $p < 0.005$, and n indicates the number of animals tested in each experiment. Comparison of data from two groups of mice was performed using Student's t test. Analysis of metabolic data was performed by ANCOVA, a statistical test that, in our case, evaluates whether population means of EE (our dependent variable) differ between mice of different genotype (our independent variable) while statistically controlling for the effects of body weight on EE (our covariate). The F value is the ratio of variability between groups (which, in

DOI: 10.1021/acs.biochem.5b00700
Biochemistry 2015, 54, 5605–5616

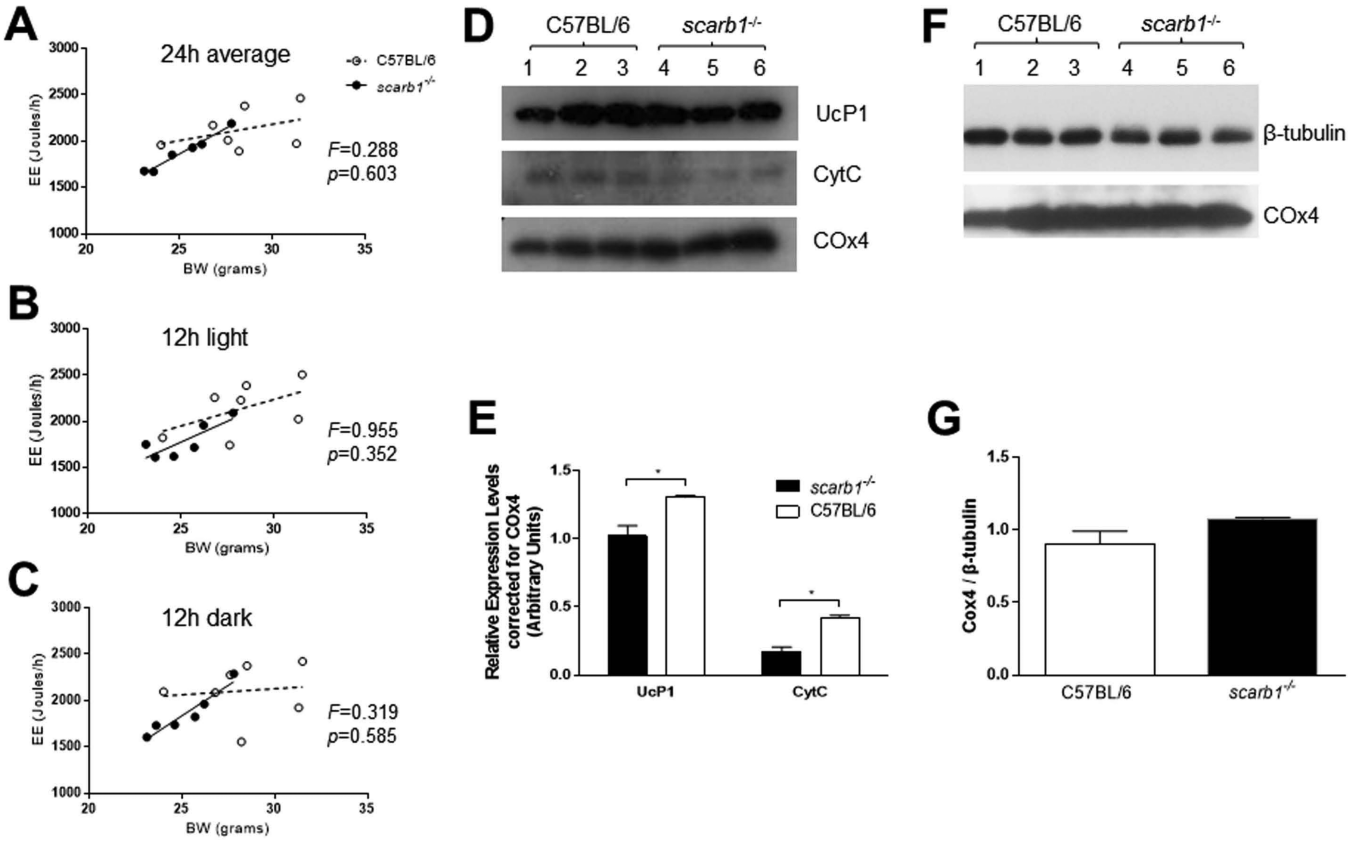

Figure 3. Metabolic analyses of *scarb1*$^{-/-}$ and C57BL/6 mice. (A–C) Linear regression plots of energy expenditure (J/h) versus mouse body weight (g) during a full day period of 24 h (12 h light/12 dark) (A), 12 h light (B), and 12 h dark (C). For each panel, ANCOVA analysis was performed, and the *F* and *p* values are indicated. (D, E) Representative western blot analysis for CytC, UcP1, and COx4 (D) and semiquantitative determination of UcP1 and CytC levels (E) in mitochondrial extracts from BAT of C57BL/6 (lanes 1–3) and *scarb1*$^{-/-}$ mice (lanes 4–6) fed a western-type diet for 24 weeks. In panel D, representative western blot data were produced from the same blot probed with the indicated antibodies. Mitochondrial protein recovery was determined by rehybridization of the membrane with the COx4 antibody. In the bar graph of panel E, all values were normalized to the signal for COx4. All data are expressed as the mean ratio of the arbitrary units of UcP1 and CytC over the arbitrary units of COx4. (F, G) Representative western blot analysis for COx4 in total BAT lysates (F) and a semiquantitative determination of COx4 levels normalized for β-tubulin (G). All values represent the mean ± SEM; * indicates $p < 0.05$.

our case, relates to genotype differences) divided by the variability within group (which, in our case, relates to body weight differences) and is a measure of the difference in EE between groups. The higher the *F* value, the higher the difference between groups when corrected for body weight; the *p* value indicates the statistical significance of the observed differences. In cases where we studied a dependent variable when the same subject was measured multiple times under a number of different conditions, we performed a two-way repeated measures ANOVA. The results of this analysis are shown in Table 1. All statistical tests were performed using SPSS software (IBM SPSS Statistics for Windows, version 22.0).

RESULTS

Effects of SR-BI Deficiency on Mouse Metabolic Phenotype. Hematoxylin and eosin (H&E) staining of liver sections revealed that control C57BL/6 mice exhibited remarkable steatosis of the macrovesicular type, characterized by excessive diffuse accumulation of lipids within hepatocytes (Figure 1A). In contrast, mice deficient in SR-BI did not show any significant distortion of liver microscopic morphology or hepatic accumulation of lipids (Figure 1B). In agreement with these data, staining of hepatic sections with reticulin showed that NAFLD was much more progressed and resulted in a significant disruption of the normal architecture of the liver extracellular reticulin fibrils in C57BL/6 mice fed a western-type diet for 24 weeks (Figure 1C), whereas *scarb1*$^{-/-}$ mice did not show any significant distortion of hepatic tissue architecture (Figure 1D). Statistical analysis following histomorphometric evaluation of the H&E sections confirmed that the number of lipid droplets within hepatocytes was significantly reduced in the *scarb1*$^{-/-}$ mice as compared to that in C57BL/6 mice (p = 0.00414) (Figure 1E).

Biochemical measurement of total hepatic TG and cholesterol content showed that the observed steatosis of C57BL/6 mice was due to excess accumulation of TG rather than cholesterol (Figure 1F,G). Specifically, C57BL/6 mice had a hepatic TG content of 142 ± 1 mg per gram of hepatic tissue and a cholesterol content of only 18 ± 3 mg per gram of hepatic tissue (Figure 2F,G), whereas *scarb1*$^{-/-}$ mice had a significantly lower TG content of 50 ± 5 mg per gram of hepatic tissue (p = 0.0020 compared to C57BL/6 mice) and a cholesterol content of 26 ± 1 mg per gram of hepatic tissue (p = 0.0546 compared to C57BL/6 mice) (Figure 2F,G).

Mice deficient in SR-BI were also resistant to body weight gain. Although both mouse strains had a similar body weight (22.7 ± 0.9 g for C57BL/6 vs 22.0 ± 0.7 g for *scarb1*$^{-/-}$) and

DOI: 10.1021/acs.biochem.5b00700
Biochemistry 2015, 54, 5605–5616

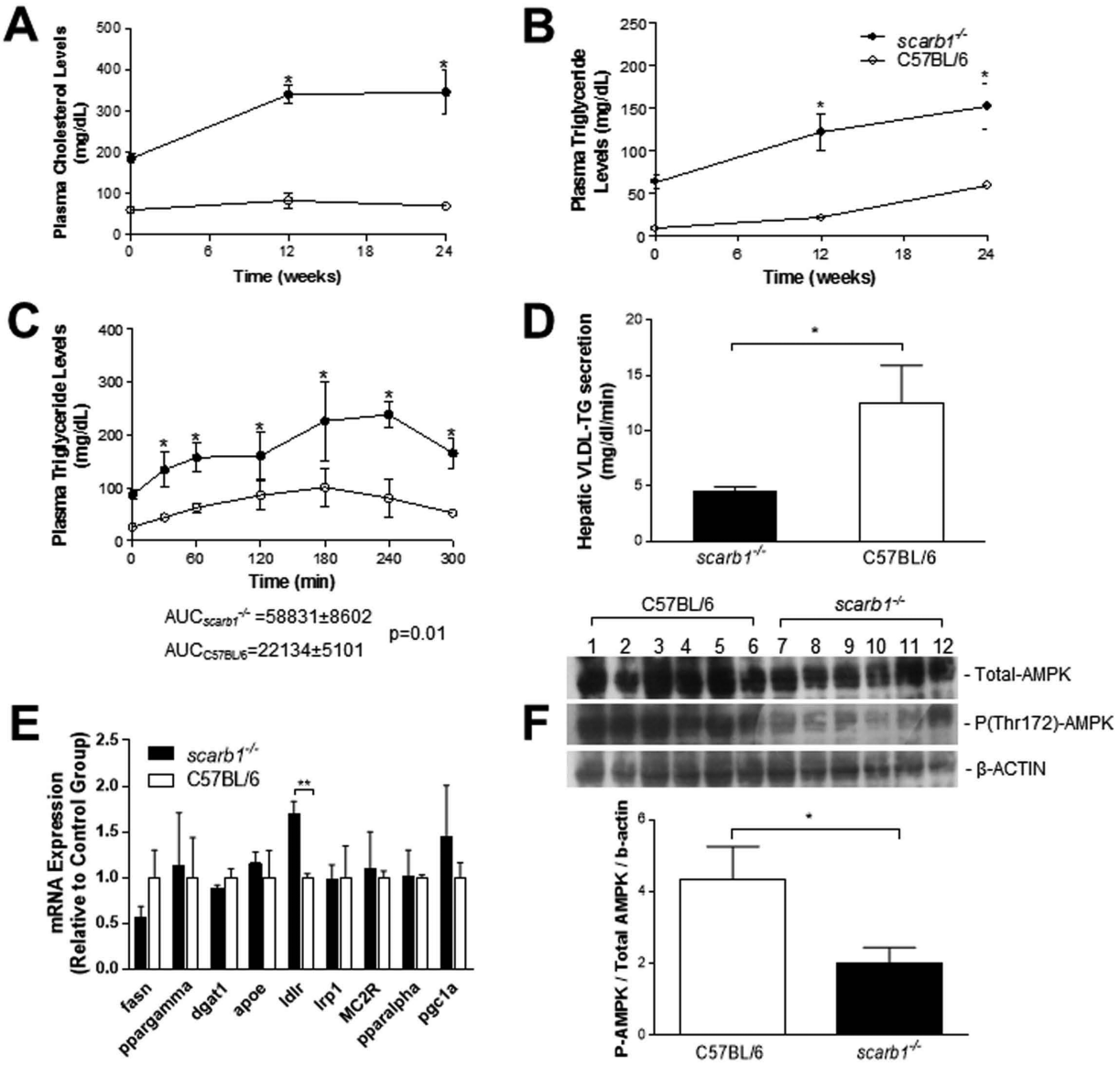

Figure 4. Biochemical parameters of *scarb1*$^{-/-}$ and C57BL/5 mice fed a western-type diet for 24 weeks. (A, B) Plasma cholesterol and triglyceride levels of *scarb1*$^{-/-}$ (●) and C57BL/6 (○) mice during the course of the experiment. (C) Representative analysis of the rate of postprandial TG clearance in *scarb1*$^{-/-}$ (●) and C57BL/6 (○) mice at week 24 of the experiment. AUC is expressed in mg/dL/min. (D) Representative analysis of the rate of hepatic VLDL-TG secretion in *scarb1*$^{-/-}$ (●) and C57BL/6 (○) mice at week 24 of the experiment. (E) Relative gene expression levels of *apoe*, *dgat-1*, *fasn*, *ldlr*, *lrp1*, *mc2r*, *pgc1a*, *pparalpha*, and *ppargamma* in the liver from *scarb1*$^{-/-}$ (■) and C57BL/6 (□) mice at week 24 of the experiment. (F) Representative western blots for AMPK, phospho(Thr172)-AMPK, and β-actin (as an internal control) in hepatic extracts of *scarb1*$^{-/-}$ (■) (lanes 7−12) and C57BL/6 (□) mice (lanes 1−6) isolated at week 24 of the experiment. Data were produced from the same blot probed with the indicated antibodies. Protein recovery from liver extracts was determined by rehybridization of the membrane with the β-actin antibody. The bar graph is the semiquantitative analysis of the western blot data normalized for β-actin. Bars represent the mean ratio of the arbitrary units of AMPK and phospho(Thr172)-AMPK over the arbitrary units of β-actin. All values represent the mean ± SEM; * indicates $p < 0.05$, and ** indicates $p < 0.005$.

lean body mass (19.6 ± 0.8 g for C57BL/6 vs 19.2 ± 1.0 g for *scarb1*$^{-/-}$) at the beginning of the experiment, significant differences appeared when mice were fed a western-type diet. As expected,[23] C57BL/6 mice showed a progressive increase in body weight during the course of the experiment (Figure 1H), reaching 29.7 ± 1.7 g at week 24 ($p < 0.05$). In contrast, *scarb1*$^{-/-}$ mice appeared to be resistant to diet-induced obesity (Figure 1H), reaching 24.0 ± 1.1 g ($p = 0.27$) at week 24, although they exhibited increased food intake (5.4 ± 0.3 g/day/mouse for *scarb1*$^{-/-}$ vs 3.8 ± 0.2 g/day/mouse for C57BL/6, $p = 0.0005$) (Figure 1I).

GTT indicated that only *scarb1*$^{-/-}$ mice maintained their normal ability to respond to intraperitoneal glucose administration at week 24 of the experiment. Specifically, at week 0, *scarb1*$^{-/-}$ mice showed a better response to intraperitoneal administration of glucose ($AUC_{scarb1^{-/-}}$ = 22 694 ± 2685 mg/dL/min vs $AUC_{C57BL/6}$ = 29 409 ± 3644 mg/dL/min, $p = 0.03$) (Figure 2A). Similarly, at week 24, *scarb1*$^{-/-}$mice maintained normal fasting glucose levels of 59 ± 4 mg/dL and displayed a far better response to intraperitoneal glucose administration than C57BL/6 mice ($AUC_{scarb1^{-/-}}$ = 15 298 ± 1482 mg/dL/min vs $AUC_{C57BL/6}$ = 36 968 ± 4883 mg/dL/min, $p = 0.002$)

DOI: 10.1021/acs.biochem.5b00700
Biochemistry 2015, 54, 5605−5616

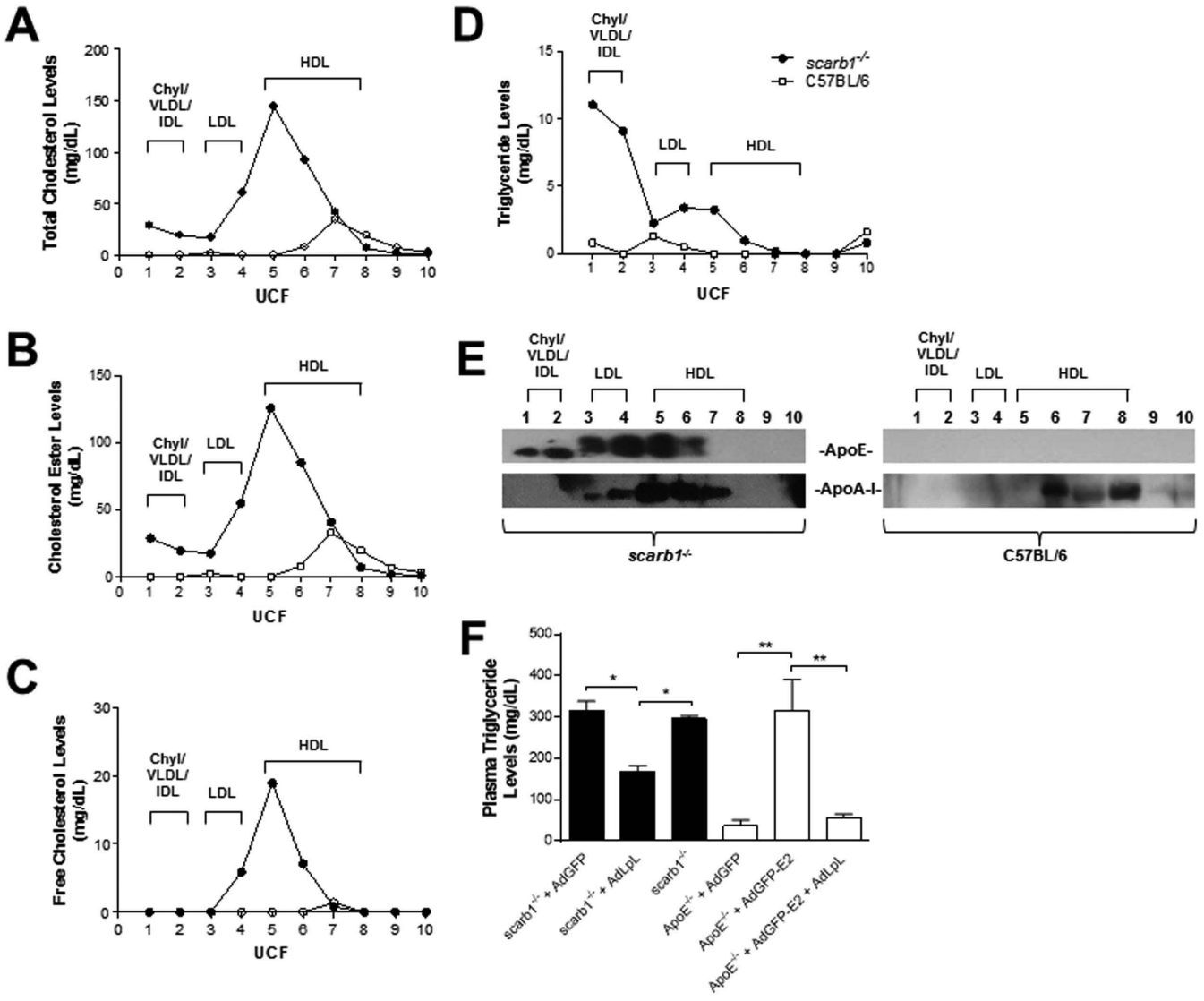

Figure 5. Lipid and apolipoprotein levels in *scarb1*$^{-/-}$ and C57BL/5 mice fed a western type diet. (A–D) Cholesterol (A), CE (B), free cholesterol (C), and TG (D) content of the various lipoprotein fractions following UCF purification of lipoproteins from *scarb1*$^{-/-}$ (●) and C57BL/6 (○) mice fed a western-type diet for 24 weeks. The position of the different lipoproteins is indicated. (E) Representative western blots for ApoE and ApoA-I in UCF lipoprotein fractions from *scarb1*$^{-/-}$ and C57BL/6 mice fed a western-type diet for 24 weeks. The position of the different lipoproteins is indicated. (F) Plasma TG levels of *scarb1*$^{-/-}$ mice fed a western-type diet for 10 weeks and then treated for 3 days with a human LpL-expressing adenovirus, AdLpL, or control adenovirus, AdGFP. As a control, to verify the expression of LpL following adenovirus infection, ApoE$^{-/-}$ mice were also treated with AdLpL in the presence or absence of AdGFP-E2 adenovirus.

(Figure 2B), which also had elevated fasting plasma glucose of 105 ± 19 mg/dL (p = 0.039 compared to week 0). The better response of *scarb1*$^{-/-}$ mice to glucose was also confirmed using two-way repeated measures ANOVA, as summarized in Table 1.

Scarb1$^{-/-}$ mice also had a higher sensitivity to exogenous insulin at both weeks 0 ($AUC_{scarb1^{-/-}}$ = 2831 ± 487 mg/dL/min vs $AUC_{C57BL/6}$ = 4590 ± 349 mg/dL/min, p = 0.02) (Figure 2C) and 24 ($AUC_{scarb1^{-/-}}$ = 3480 ± 383 mg/dL/min vs $AUC_{C57BL/6}$ = 5168 ± 325 mg/dL/min, p = 0.01) (Figure 2D). The better response of *scarb1*$^{-/-}$ mice to insulin was also confirmed using a two-way repeated measures ANOVA, as shown in Table 1. Measurement of plasma insulin levels during GTT indicated that *scarb1*$^{-/-}$ mice require significantly lower plasma insulin levels to produce an improved response during GTT ($AUC_{scarb1^{-/-}}$ = 71 ± 2 ng/mL/min vs $AUC_{C57BL/6}$ = 251 ± 5 ng/mL/min, p = 0.01) (Figure 2E). Two-way repeated measures ANOVA confirmed that *scarb1*$^{-/-}$ mice secreted significantly less insulin than C57BL/6 mice during GTT (Table 1).

Deficiency in SR-BI Has No Apparent Effect on Energy Expenditure and Mitochondrial Function. In an effort to determine whether differences in EE may be a causal factor for the phenotypic differences between the two mouse groups, indirect calorimetry analysis was performed. We chose to characterize our mice at the beginning of the experiment (week 0) on the basis of the recommendations of Tschop and co-workers[33] that such metabolic phenotyping should be ideally performed at week 0 of the experiment, when body weight and lean body mass are similar between groups of mice. Average EE was 1881 ± 80 J/h for *scarb1*$^{-/-}$ mice and 2122 ± 85 J/h for C57BL/6 mice (p = 0.066). ANCOVA analysis indicated that, when controlled for body weight, *scarb1*$^{-/-}$ and C57BL/6 mouse groups exhibit similar EE (F = 0.228, p = 0.603; n = 6

DOI: 10.1021/acs.biochem.5b00700
Biochemistry 2015, 54, 5605–5616

for *scarb1*$^{-/-}$ and $n = 7$ for control C57BL/6 mice) (Figure 3A). Similarly, no significant difference was determined in the average RER between the two groups (0.862 ± 0.05 for *scarb1*$^{-/-}$ and 0.882 ± 0.047 for C57BL/6, $p = 0.735$), consistent with the fact that animals in both groups consumed the same diet and similar types of fuel as energy. Separate ANCOVA analysis of the EE values collected during the 12h light cycle (7.00 am to 6.59 pm, $F = 0.955$, $p = 0.352$; $n = 6$ for *scarb1*$^{-/-}$ and $n = 7$ for control C57BL/6 mice) (Figure 3B) and the 12 h dark cycle (7.00 pm to 6.59 am, $F = 0.319$, $p = 0.585$; $n = 6$ for *scarb1*$^{-/-}$ and $n = 7$ for control C57BL/6 mice) (Figure 3C) indicated that in both cycles there was no difference between *scarb1*$^{-/-}$ and C57BL/6 mice, further suggesting that there are no variations in physical activity between the two mouse groups.

Western blot analysis of mitochondrial lysates from brown adipose tissue (BAT) showed reduced CytC levels in *scarb1*$^{-/-}$ mice, suggesting reduced mitochondrial oxidative phosphorylation function (Figure 3D,E). Similarly, reduced uncoupling of substrate oxidative phosphorylation from respiration was observed between strains of mice, as measured by the levels of expression of UcP1 (Figure 3D,E). UcP1 and CytC levels were normalized to COx4 levels, an internal loading standard for mitochondrial protein (Figure 3E). No increase in the number of mitochondria in BAT of *scarb1*$^{-/-}$ mice was found, as indicated by the level of COx4 in total lysates (Figure 3F,G)

Effects of SR-BI Deficiency on Plasma Lipid Levels and Lipoprotein Metabolism Kinetics. *Scarb1*$^{-/-}$ mice showed a significant increase in their plasma cholesterol and TG at the end of the study. Specifically, at week 24, their plasma cholesterol was 345.6 ± 52.1 mg/dL, compared to the initial levels of 184.7 ± 11.4 mg/dL at week 0 (Figure 4A). Similarly, their plasma TG was 152.3 ± 26.3 mg/dL, compared to 63.9 ± 8.6 mg/dL at week 0 ($p = 0.00001$) (Figure 4B). In contrast, C57BL/6 mice on a high-fat diet for 24 weeks had slightly increased fasting cholesterol levels of 70 ± 5.5 mg/dL, as compared to their starting levels of 60.7 ± 4.1 mg/dL at week 0 ($p = 0.0059$) (Figure 4A), whereas their plasma TG remained normal (59.7 ± 3.9 mg/dL at week 24 vs 8.7 ± 1.2 mg/dL at week 0) (Figure 4B). Two-way repeated measures ANOVA analysis confirmed the differences between *scarb1*$^{-/-}$ and C57BL/6 mice (Table 1).

We next investigated whether differences in the rates of postprandial TG clearance could account for the observed differences in liver lipid content. As shown in Figure 4C, *scarb1*$^{-/-}$ mice displayed much slower kinetics of postprandial TG clearance ($AUC_{scarb1^{-/-}}$ = 58 831 ± 8602 mg/dL/min vs $AUC_{C57BL/6}$ = 22 134 ± 5101, $p = 0.01$) (Figure 4C).

Another mechanism that could explain the observed phenotypic differences is the rate of secretion of hepatic VLDL-TG into circulation. We found that *scarb1*$^{-/-}$ mice had a secretion rate of 4.56 ± 0.41 mg/dL/min, compared to 12.52 ± 1.33 mg/dL/min for C57BL/6 mice ($p = 0.0161$) (Figure 4D).

In an effort to determine if *de novo* biogenesis of FFA and TG is a factor in the observed phenotypic differences between the two strains of mice, we measured the mRNA levels of key lipogenic enzymes, *fasn*, *dgat1*, and *ppargamma*, by RT-PCR as well as *apoe*, *ldlr*, and *lrp1*. No differences were found in the relative expression of *fasn*, *dgat1*, *ppargamma*, *apoe*, and *lrp1* between strains of mice (Figure 4E). Only *ldlr* gene expression was increased in *scarb1*$^{-/-}$ mice. In addition, western blot analysis of hepatic extracts showed that SR-BI deficiency is associated with reduced AMPK activity, as indicated by the ratio of phosphorylated at Thr172 AMPK (phospho-AMPK) versus total AMPK present in the livers of *scarb1*$^{-/-}$ mice (Figure 4F). Similarly, fatty acid oxidation does not appear to be affected between strains of mice, as indicated by the lack of difference in the expression levels of *pparalpha* and *pgc1a* (Figure 4E). In an effort to identify any potential involvement of melanocortin receptor 2 (MC2R) in the observed phenotype, we also analyzed *mc2r* hepatic mRNA levels. No differences were observed between *scarb1*$^{-/-}$ and C57BL/6 mice (Figure 4E).

Deficiency in SR-BI Results in Accumulation of ApoE-Containing TG-Rich Lipoproteins and Inhibition of Lipoprotein Lipase. Since *scarb1*$^{-/-}$ mice display impaired postprandial TG clearance, we next sought to investigate if the effects of SR-BI deficiency on hepatic TG deposition are due to its function as a modulator of apolipoprotein and lipoprotein metabolism in plasma. To this effect, we determined total cholesterol, TG, free cholesterol, and CE in the different lipoprotein fractions. This analysis revealed significant differences in the cholesterol and TG lipoprotein profiles of *scarb1*$^{-/-}$ and C57BL/6 mice fed a western-type diet for 24 weeks (Figure 5A,D). Notably, *scarb1*$^{-/-}$ mice had significantly higher levels of TG-rich chylomicrons, VLDL, IDL, and LDL in their plasma (Figure 5D). Another striking difference was that in *scarb1*$^{-/-}$ mice cholesterol was significantly elevated in all lipoprotein fractions, although it was primarily accumulated in lipid-rich large α-HDL particles (Figure 5A). Most of the cholesterol was esterified (Figure 5B), with only small amounts of free cholesterol present mainly in HDL and, to a lesser extent, LDL fractions (Figure 5C).

Determination of ApoE and ApoA-I by western blotting in various lipoprotein fractions revealed that in *scarb1*$^{-/-}$ mice fed a western-type diet for 24 weeks there was a significant accumulation of ApoE in TG-rich lipoproteins (chylomicrons/VLDL/IDL) and in LDL (Figure 5E). The presence of increased levels of ApoE correlated with elevated TG levels in these fractions (Figure 5D). In addition to ApoE, *scarb1*$^{-/-}$ mice also exhibited increased ApoA-I accumulation mainly in HDL (Figure 5E) and a shift of ApoA-I toward lighter HDL fractions, whereas substantial amounts of ApoA-I were also found in LDL fractions. No effect on *apoe* expression was observed between *scarb1*$^{-/-}$ and C57BL/6 mice (Figure 4E), suggesting that the increase in plasma ApoE protein levels in *scarb1*$^{-/-}$ mice is not a result of increased hepatic gene expression.

We have shown previously that ApoE overexpression results in combined dyslipidemia (hypercholesterolemia and hypertriglyceridemia) and that overexpression of LpL by adenovirus-mediated gene transfer ameliorates dyslipidemia and corrects the plasma lipoprotein profile.[34] Given that ApoE is a potent inhibitor of plasma LpL activity[35,36] and that inhibition of LpL is well-known to prevent an increase in hepatic triglyceride and development of NAFLD,[37−39] we next hypothesized that elevated plasma ApoE levels in *scarb1*$^{-/-}$ mice may correlate with limited plasma LpL activity. If this was the case, then overexpression of LpL would lift the block on lipolysis, allowing plasma triglycerides to be effectively cleared. To test this hypothesis, we overexpressed LpL by adenovirus-mediated *lpl* gene transfer as a means to overcome the presumed inhibitory effect of ApoE on LpL, as done previously.[40] Indeed, *scarb1*$^{-/-}$ mice fed a western-type diet for 10 weeks received either 5×10^8 pfu of an adenovirus expressing human LpL (Ad-LpL)[32] or 5×10^8 pfu of an empty AdGFP adenovirus, as a control. As

DOI: 10.1021/acs.biochem.5b00700
Biochemistry 2015, 54, 5605−5616

shown in Figure 5F, LpL overexpression resulted in a substantial reduction in plasma TG levels in these mice 3 days following infection, confirming our hypothesis. As a control, to verify the activity of LpL *in vivo*, ApoE-deficient mice infected with 2×10^9 pfu of an ApoE2-expressing adenovirus (AdGFP-E2) were coinfected with either 5×10^8 pfu of Ad-LpL or 5×10^8 pfu of the empty AdGFP adenovirus. As expected, plasma triglyceride levels of mice expressing ApoE2 were significantly increased on day 3 following infection, whereas mice expressing both ApoE2 and LpL had normal plasma triglyceride levels, as shown previously,[32] confirming the *in vivo* activity of LpL.

DISCUSSION

In the present study, we found that *scarb1*$^{-/-}$ mice are resistant to hepatic lipid deposition even though they consume more food than WT mice (Figure 1I) and efficiently clear postprandial TG, albeit at a reduced rate (Figure 4C). It has been shown previously that deficiency in SR-BI does not affect intestinal lipid absorption,[41] suggesting that differences in intestinal uptake of dietary lipids between strains of mice may not be a factor in the observed phenotype. Similarly, the reduced hepatic lipid deposition in *scarb1*$^{-/-}$ mice could not be attributed to increased mitochondrial metabolic activity in BAT (Figure 3D,E). In a further effort to explain the resistance of *scarb1*$^{-/-}$ mice to hepatic lipid deposition, we measured by indirect calorimetry whole-animal EE, which reflects the composite activity of all metabolic tissues of the mouse (Figure 3A−C). Again, this analysis did not reveal any significant differences in the EE between the two strains of mice. Similarly, our gene expression analysis indicated reduced hepatic FFA synthesis in mice lacking SR-BI (Figure 4E). The reduced activation of AMPK, as shown by the relative amount of phospho-AMPK present in the livers of *scarb1*$^{-/-}$ mice (Figure 4F), suggested that AMPK-activated hepatic FFA catabolism may not explain the observed phenotype either. Indeed, fatty acid oxidation does not appear to be affected between strains of mice, as indicated by the lack of difference in the expression levels of *pparalpha* and *pgc1a* (Figure 4E). Taken together, these data suggest that hepatic FFA and TG metabolism cannot account for the observed phenotype in *scarb1*$^{-/-}$ mice, leaving direct dietary lipid uptake from plasma as the major contributor. Therefore, we next investigated if the effects of SR-BI deficiency on hepatic TG deposition are due to its function as a modulator of apolipoprotein and lipoprotein metabolism in plasma.

Previous reports in the literature showed that the hypercholesterolemia of *scarb1*$^{-/-}$ mice fed a chow diet is primarily due to accumulation of HDL-C (mainly CE) in circulation because of its impaired clearance.[42] This was confirmed in our study by the elevated ApoA-I, total cholesterol, and CE levels in HDL fractions (Figure 5E). However, we also found that the lack of functional SR-BI resulted in a substantial accumulation of cholesterol and ApoE in chylomicrons/VLDL/IDL and LDL following feeding a western-type diet for 24 weeks (Figure 5E). A similar but lower accumulation of ApoE has been previously seen in *scarb1*$^{-/-}$ mice fed a chow diet.[13] Of note, our data indicate a significant accumulation of ApoE not only in TG-rich lipoproteins but also in large HDL fractions. Similarly, ApoA-I accumulates in LDL fractions, in addition to HDL fractions (Figure 5E). Since under normal conditions (a) LDL contains no ApoA-I, (b) HDL contains a small amount of ApoE, and (c) ApoA-I is present solely in HDL, the observed ApoA-I and ApoE lipoprotein distribution in *scarb1*$^{-/-}$ mice suggests the existence of very large CE-rich HDL particles that float in the LDL fraction (Figure 5).

Under normal conditions, steady-state plasma ApoE levels in WT mice remain very low due to the efficient clearance of ApoE-containing lipoproteins by Ldlr. In addition, it is well-established that hepatic VLDL-TG secretion is proportional to hepatic ApoE synthesis.[43−46] Since *scarb1*$^{-/-}$ mice displayed a reduced rate of hepatic VLDL-TG secretion (Figure 4D) and similar *apoe* gene expression levels compared to those in C57BL/6 mice (Figure 4E), the increase in steady-state plasma ApoE levels in these mice must be due to impaired clearance of ApoE-containing TG-rich lipoproteins, as seen previously.[40] Indeed, analysis of the kinetics of postprandial TG clearance showed that the lack of SR-BI may significantly delay the clearance of TG-rich lipoproteins from plasma (Figure 4C). The impaired clearance of ApoE-containing TG-rich lipoproteins observed in *scarb1*$^{-/-}$ mice could be due to either reduced *ldlr* and/or *lrp1* expression or inefficient LpL-mediated lipolysis of TG-rich lipoproteins in circulation that prevent their efficient binding to these ApoE receptors.

Our data show that *Ldlr* expression is increased in *scarb1*$^{-/-}$ mice fed a western-type diet for 24 weeks, whereas *lrp1* expression remains unchanged (Figure 4E), leaving inefficient lipolysis as the sole possibility for the increased levels of ApoE-containing TG-rich lipoproteins in *scarb1*$^{-/-}$ mice. Our data, indeed, confirm that LpL activity is a limiting step in the observed hypertriglyceridemia. LpL activity is important not only for the production of lipoprotein remnants but also for the release of free fatty acids that eventually will be converted to triglycerides in the liver and peripheral tissues. This is a key mechanistic observation in our study since reduced plasma LpL correlates with significantly impaired dietary triglyceride deposition to the liver.[37−39] Since the natural tropism of the adenovirus used in the study is the liver, it is possible that the LpL expressed following adenovirus infection could also act intracellularly within liver cells. However, the profound reduction in plasma triglyceride levels observed in *scarb1*$^{-/-}$ mice infected with AdLpL further confirms the activity of ectopic LpL in circulation.

A previous *in vitro* study suggested that LpL may act as a bridging molecule that promotes the selective uptake of cholesterylesters from both LDL and HDL independently of SR-BI expression and LpL enzymatic activity.[47] However, more recent *in vivo* work by Hu et al.[48] showed that in the absence of Lrpl, Ldlr, and Vldlr, hepatic uptake of triglyceride-rich lipoproteins in mice is regulated by LpL activity, is independent of the bridging function of LpL, and involves SR-BI. In the absence of these three ApoE receptors, blocking SR-BI ablated the hepatic clearance of triglyceride-rich lipoproteins that was normally promoted by LpL activity. On the basis of this work, the apparent clearance of triglyceride-rich lipoproteins that we observed in *scarb1*$^{-/-}$ mice infected with AdLpL (Figure 5F) is due to increased plasma LpL lipolytic activity and not to the previously proposed indirect role of LpL as a bridging molecule. In the present study, we were not able to observe any significant difference in hepatic lipid content between AdLpL-infected and AdGFP-infected *scarb1*$^{-/-}$ mice (data not shown), a finding that was expected due to the short duration of adenovirus-mediated LpL expression.

Obviously, the inability of the liver in *scarb1*$^{-/-}$ mice to uptake HDL lipids from circulation is a key contributor to the observed hepatic phenotype of these mice and likely is related

DOI: 10.1021/acs.biochem.5b00700
Biochemistry 2015, 54, 5605−5616

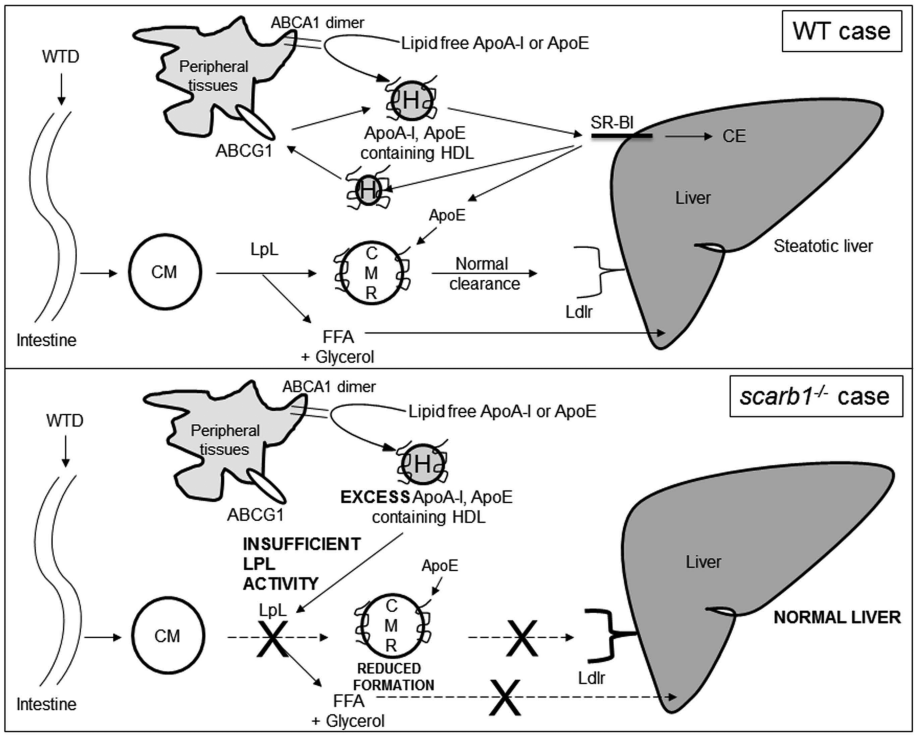

Figure 6. Schematic representation of the proposed effects of SR-BI deficiency on postprandial lipoprotein metabolism and hepatic lipid deposition. In wild-type (WT) mice (upper panel), normal SR-BI activity results in physiological plasma ApoE levels and LpL activity. However, feeding *scarb1*$^{-/-}$ mice a high-fat diet for 24 weeks (lower panel) results in the gradual accumulation of HDL-ApoE that ultimately results in insufficient LpL activity in circulation. In response, plasma TG levels increase and subsequent Ldlr-mediated clearance of ApoE-containing TG-rich lipoproteins is impaired, despite a compensatory increase in hepatic Ldlr expression. Eventually, this leads to inhibition of dietary lipid shuttling to the liver and prevention of diet-induced NAFLD development. WTD, western-type diet; CM, chylomicrons; CMR, chylomicron remnants; H, HDL; LpL, lipoprotein lipase; FFA, free fatty acids; CE, cholesteryl esters.

to their resistance to hyperglycemia. *Scarb1*$^{-/-}$ mice on a chow diet have elevated ACTH levels,[49,50] and recent data indicate that expression of *mc2r* in white adipose tissue plays a significant lipolytic role.[51] However, analysis of hepatic *mc2r* expression levels did not reveal any significant differences between *scarb1*$^{-/-}$ and C57BL/6 mice (Figure 4E). Therefore, a highly likely scenario supported by our data is that, following feeding a high-fat diet for 24 weeks, the gradually accumulating HDL-ApoE ultimately results in insufficient LpL activity in circulation, possibly due to LpL inhibition by ApoE.[35,36] This results in elevated plasma TG levels due to impaired lipolysis and subsequent Ldlr-mediated clearance of ApoE-containing TG-rich lipoproteins, despite a compensatory increase in hepatic *ldlr* expression, possibly in a fashion similar to statins. Eventually, this leads to inhibition of dietary lipid shuttling to the liver and prevention of diet-induced NAFLD development (Figure 6).

HDL is a heterogeneous mixture of lipoprotein particles that differ in size, shape, lipid, and apoprotein composition,[52] and variations in apolipoprotein and lipid content of these particles set the basis for the functional heterogeneity of HDL.[53−55] In the present study, we show that lack of SR-BI, the final molecular partner of plasma HDL's metabolic pathway, prevents the development and severity of hepatic lipid deposition and associated glucose intolerance. Combining this observation with our previously published work in *apoa1*$^{-/-}$ and *lcat*$^{-/-}$ mice,[20,21] it appears that select protein components of HDL's metabolic pathway have distinct and even opposing effects on hepatic lipid deposition. Our findings further suggest that a change of function of HDL-related proteins, rather than HDL-C levels, may be crucial for defining susceptibility to NAFLD.

■ ASSOCIATED CONTENT

Supporting Information

The Supporting Information is available free of charge on the ACS Publications website at DOI: 10.1021/acs.biochem.5b00700.

Genotyping *scarb*$^{-/-}$ mice (PDF).

■ AUTHOR INFORMATION

Corresponding Author

*Tel: +302610969120. Fax: +302610996103. E-mail: kkypreos@med.upatras.gr.

Funding

The work was financially supported by the action "Excellence" of the Operational Program "Education and Lifelong Learning" (Action's Beneficiary: Hellenic General Secretariat for Research and Technology), which is cofinanced by the European Social Fund (ESF) and the Greek State (grant no. 248, awarded to K.E.K.). This work was part of the activities of the intramural research network MetSNet (www.metsnet.gr) of the University of Patras. Dr. Caterina Constantinou is a Research Fellow supported by a "Siemens-Excellence" award financed by the Hellenic State Scholarships Foundation (IKY).

Notes

The authors declare no competing financial interest.

DOI: 10.1021/acs.biochem.5b00700
Biochemistry 2015, 54, 5605−5616

■ ABBREVIATIONS

Ad, adenovirus; AdGFP, recombinant attenuated adenovirus expressing green fluorescent protein; AdGFP-E2, recombinant attenuated adenovirus expressing the human ApoE2 isoform and GFP under the independent control of separate CMV promoters; AdLpL, recombinant attenuated adenovirus expressing human lipoprotein lipase; ApoA-I, apolipoprotein A-I; ApoA-II, apolipoprotein A-II; ApoB, apolipoprotein B; ApoE, apolipoprotein E; ApoE2, human apolipoprotein E isoform 2; ApoE$^{-/-}$, ApoE deficient; AUC, area under the curve; CE, cholesteryl esters; CMV, cytomegalovirus; *dgat1*, diacylglycerol acyltransferase isoform 1 gene; EE, energy expenditure; GFP, green fluorescent protein; GTT, glucose tolerance test; HDL-C, HDL cholesterol; IDL, intermediate density lipoprotein; IST, insulin sensitivity test; LDL, low-density lipoprotein; LpL, lipoprotein lipase; MOI, multiplicity of infection; *mc2r*, melanocortin receptor 2 gene; NAFLD, nonalcoholic fatty liver disease; oxLDL, oxidized LDL; pfu, plaque-forming unit; *pgc1a*, peroxisome proliferator-activated receptor gamma coactivator 1-alpha gene; *pparalpha*, peroxisome proliferator-activated receptor alpha gene; *ppargamma*, peroxisome proliferator-activated receptor gamma gene; RCT, reverse cholesterol transport; *rps18*, 40S ribosomal protein S18 gene; *scarb1*, scavenger receptor class B member I gene; *scarb1*$^{-/-}$, SR-BI-deficient animals; SR-BI, scavenger receptor class B member I; SR-BI-Tg, SR-BI transgenic mice; TG, triglycerides; UCF, density gradient ultracentrifugation; VLDL, very low density lipoprotein; WT, wild type

■ REFERENCES

(1) Krieger, M. (1999) Charting the fate of the "good cholesterol": identification and characterization of the high-density lipoprotein receptor SR-BI. *Annu. Rev. Biochem. 68*, 523−558.

(2) Acton, S., Rigotti, A., Landschulz, K. T., Xu, S., Hobbs, H. H., and Krieger, M. (1996) Identification of scavenger receptor SR-BI as a high density lipoprotein receptor. *Science 271*, 518−520.

(3) Landschulz, K. T., Pathak, R. K., Rigotti, A., Krieger, M., and Hobbs, H. H. (1996) Regulation of scavenger receptor, class B, type I, a high density lipoprotein receptor, in liver and steroidogenic tissues of the rat. *J. Clin. Invest. 98*, 984−995.

(4) Acton, S. L., Scherer, P. E., Lodish, H. F., and Krieger, M. (1994) Expression cloning of SR-BI, a CD36-related class B scavenger receptor. *J. Biol. Chem. 269*, 21003−21009.

(5) Swarnakar, S., Temel, R. E., Connelly, M. A., Azhar, S., and Williams, D. L. (1999) Scavenger receptor class B, type I, mediates selective uptake of low density lipoprotein cholesteryl ester. *J. Biol. Chem. 274*, 29733−29739.

(6) de la Llera-Moya, M., Connelly, M. A., Drazul, D., Klein, S. M., Favari, E., Yancey, P. G., Williams, D. L., and Rothblat, G. H. (2001) Scavenger receptor class B type I affects cholesterol homeostasis by magnifying cholesterol flux between cells and HDL. *J. Lipid Res. 42*, 1969−1978.

(7) Tall, A. R. (2008) Cholesterol efflux pathways and other potential mechanisms involved in the athero-protective effect of high density lipoproteins. *J. Intern. Med. 263*, 256−273.

(8) Berge, K. E., Tian, H., Graf, G. A., Yu, L., Grishin, N. V., Schultz, J., Kwiterovich, P., Shan, B., Barnes, R., and Hobbs, H. H. (2000) Accumulation of dietary cholesterol in sitosterolemia caused by mutations in adjacent ABC transporters. *Science 290*, 1771−1775.

(9) Gillotte-Taylor, K., Boullier, A., Witztum, J. L., Steinberg, D., and Quehenberger, O. (2001) Scavenger receptor class B type I as a receptor for oxidized low density lipoprotein. *J. Lipid Res. 42*, 1474−1482.

(10) Sun, B., Boyanovsky, B. B., Connelly, M. A., Shridas, P., van der Westhuyzen, D. R., and Webb, N. R. (2007) Distinct mechanisms for OxLDL uptake and cellular trafficking by class B scavenger receptors CD36 and SR-BI. *J. Lipid Res. 48*, 2560−2570.

(11) Kozarsky, K. F., Donahee, M. H., Rigotti, A., Iqbal, S. N., Edelman, E. R., and Krieger, M. (1997) Overexpression of the HDL receptor SR-BI alters plasma HDL and bile cholesterol levels. *Nature 387*, 414−417.

(12) Wang, N., Arai, T., Ji, Y., Rinninger, F., and Tall, A. R. (1998) Liver-specific overexpression of scavenger receptor BI decreases levels of very low density lipoprotein ApoB, low density lipoprotein ApoB, and high density lipoprotein in transgenic mice. *J. Biol. Chem. 273*, 32920−32926.

(13) Rigotti, A., Trigatti, B. L., Penman, M., Rayburn, H., Herz, J., and Krieger, M. (1997) A targeted mutation in the murine gene encoding the high density lipoprotein (HDL) receptor scavenger receptor class B type I reveals its key role in HDL metabolism. *Proc. Natl. Acad. Sci. U. S. A. 94*, 12610−12615.

(14) Van Eck, M., Twisk, J., Hoekstra, M., Van Rij, B. T., Van der Lans, C. A., Bos, I. S., Kruijt, J. K., Kuipers, F., and Van Berkel, T. J. (2003) Differential effects of scavenger receptor BI deficiency on lipid metabolism in cells of the arterial wall and in the liver. *J. Biol. Chem. 278*, 23699−23705.

(15) Marceau, P., Biron, S., Hould, F. S., Marceau, S., Simard, S., Thung, S. N., and Kral, J. G. (1999) Liver pathology and the metabolic syndrome X in severe obesity. *J. Clin. Endocrinol. Metab. 84*, 1513−1517.

(16) Marchesini, G., Brizi, M., Bianchi, G., Tomassetti, S., Bugianesi, E., Lenzi, M., McCullough, A. J., Natale, S., Forlani, G., and Melchionda, N. (2001) Nonalcoholic fatty liver disease: a feature of the metabolic syndrome. *Diabetes 50*, 1844−1850.

(17) Tilg, H., and Moschen, A. R. (2010) Evolution of inflammation in nonalcoholic fatty liver disease: the multiple parallel hits hypothesis. *Hepatology 52*, 1836−1846.

(18) Marchesini, G., Moscatiello, S., Di Domizio, S., and Forlani, G. (2008) Obesity-associated liver disease. *J. Clin. Endocrinol. Metab. 93*, S74−S80.

(19) Chalasani, N., Younossi, Z., Lavine, J. E., Diehl, A. M., Brunt, E. M., Cusi, K., Charlton, M., and Sanyal, A. J. (2012) The diagnosis and management of non-alcoholic fatty liver disease: practice Guideline by the American Association for the Study of Liver Diseases, American College of Gastroenterology, and the American Gastroenterological Association. *Hepatology 55*, 2005−2023.

(20) Karavia, E. A., Papachristou, D. J., Liopeta, K., Triantaphyllidou, I. E., Dimitrakopoulos, O., and Kypreos, K. E. (2012) Apolipoprotein A-I modulates processes associated with diet-induced nonalcoholic fatty liver disease in mice. *Mol. Med. 18*, 901−912.

(21) Karavia, E. A., Papachristou, D. J., Kotsikogianni, I., Triantafyllidou, I. E., and Kypreos, K. E. (2013) Lecithin/cholesterol acyltransferase modulates diet-induced hepatic deposition of triglycerides in mice. *J. Nutr. Biochem. 24*, 567−577.

(22) Duivenvoorden, I., Teusink, B., Rensen, P. C., Romijn, J. A., Havekes, L. M., and Voshol, P. J. (2005) Apolipoprotein C3 deficiency results in diet-induced obesity and aggravated insulin resistance in mice. *Diabetes 54*, 664−671.

(23) Karagiannides, I., Abdou, R., Tzortzopoulou, A., Voshol, P. J., and Kypreos, K. E. (2008) Apolipoprotein E predisposes to obesity and related metabolic dysfunctions in mice. *FEBS J. 275*, 4796−4809.

(24) Karavia, E. A., Papachristou, D. J., Kotsikogianni, I., Giopanou, I., and Kypreos, K. E. (2011) Deficiency in apolipoprotein E has a protective effect on diet-induced nonalcoholic fatty liver disease in mice. *FEBS J. 278*, 3119−3129.

(25) Aalto-Setala, K., Fisher, E. A., Chen, X., Chajek-Shaul, T., Hayek, T., Zechner, R., Walsh, A., Ramakrishnan, R., Ginsberg, H. N., and Breslow, J. L. (1992) Mechanism of hypertriglyceridemia in human apolipoprotein (apo) CIII transgenic mice. Diminished very low density lipoprotein fractional catabolic rate associated with increased apo CIII and reduced apo E on the particles. *J. Clin. Invest. 90*, 1889−1900.

(26) Kypreos, K. E., Van Dijk, K. W., van der Zee, A., Havekes, L. M., and Zannis, V. I. (2001) Domains of apolipoprotein E contributing to

DOI: 10.1021/acs.biochem.5b00700
Biochemistry 2015, 54, 5605−5616

triglyceride and cholesterol homeostasis in vivo. Carboxyl-terminal region 203−299 promotes hepatic very low density lipoprotein-triglyceride secretion. *J. Biol. Chem. 276*, 19778−19786.
(27) Constantinou, C., Mpatsoulis, D., Natsos, A., Petropoulou, P. I., Zvintzou, E., Traish, A. M., Voshol, P. J., Karagiannides, I., and Kypreos, K. E. (2014) The low density lipoprotein receptor modulates the effects of hypogonadism on diet-induced obesity and related metabolic perturbations. *J. Lipid Res. 55*, 1434−1447.
(28) Kypreos, K. E. (2008) ABCA1 Promotes the de Novo Biogenesis of Apolipoprotein CIII-Containing HDL Particles in Vivo and Modulates the Severity of Apolipoprotein CIII-Induced Hypertriglyceridemia. *Biochemistry 47*, 10491−10502.
(29) Commins, S. P., Watson, P. M., Padgett, M. A., Dudley, A., Argyropoulos, G., and Gettys, T. W. (1999) Induction of uncoupling protein expression in brown and white adipose tissue by leptin. *Endocrinology 140*, 292−300.
(30) Kobayashi, J., Applebaum-Bowden, D., Dugi, K. A., Brown, D. R., Kashyap, V. S., Parrott, C., Duarte, C., Maeda, N., and Santamarina-Fojo, S. (1996) Analysis of protein structure-function in vivo. Adenovirus-mediated transfer of lipase lid mutants in hepatic lipase-deficient mice. *J. Biol. Chem. 271*, 26296−26301.
(31) Van Dijk, K. W., van Vlijmen, B. J., van't Hof, H. B., van Der, Z. A., Santamarina-Fojo, S., van Berkel, T. J., Havekes, L. M., and Hofker, M. H. (1999) In LDL receptor-deficient mice, catabolism of remnant lipoproteins requires a high level of apoE but is inhibited by excess apoE. *J. Lipid Res. 40*, 336−344.
(32) Kypreos, K. E., Li, X., Van Dijk, K. W., Havekes, L. M., and Zannis, V. I. (2003) Molecular mechanisms of type III hyperlipoproteinemia: The contribution of the carboxy-terminal domain of ApoE can account for the dyslipidemia that is associated with the E2/E2 phenotype. *Biochemistry 42*, 9841−9853.
(33) Tschop, M. H., Speakman, J. R., Arch, J. R., Auwerx, J., Bruning, J. C., Chan, L., Eckel, R. H., Farese, R. V., Jr., Galgani, J. E., Hambly, C., Herman, M. A., Horvath, T. L., Kahn, B. B., Kozma, S. C., Maratos-Flier, E., Muller, T. D., Munzberg, H., Pfluger, P. T., Plum, L., Reitman, M. L., Rahmouni, K., Shulman, G. I., Thomas, G., Kahn, C. R., and Ravussin, E. (2012) A guide to analysis of mouse energy metabolism. *Nat. Methods 9*, 57−63.
(34) Kypreos, K. E., Van Dijk, K. W., Havekes, L. M., and Zannis, V. I. (2005) Generation of a recombinant apolipoprotein E variant with improved biological functions: hydrophobic residues (LEU-261, TRP-264, PHE-265, LEU-268, VAL-269) of apoE can account for the apoE-induced hypertriglyceridemia. *J. Biol. Chem. 280*, 6276−6284.
(35) Havel, R. J., Kotite, L., Vigne, J. L., Kane, J. P., Tun, P., Phillips, N., and Chen, G. C. (1980) Radioimmunoassay of human arginine-rich apolipoprotein, apoprotein E. Concentration in blood plasma and lipoproteins as affected by apoprotein E-3 deficiency. *J. Clin. Invest. 66*, 1351−1362.
(36) Rensen, P. C., and van Berkel, T. J. (1996) Apolipoprotein E effectively inhibits lipoprotein lipase-mediated lipolysis of chylomicron-like triglyceride-rich lipid emulsions in vitro and in vivo. *J. Biol. Chem. 271*, 14791−14799.
(37) Pardina, E., Lecube, A., Llamas, R., Catalan, R., Galard, R., Fort, J. M., Allende, H., Vargas, V., Baena-Fustegueras, J. A., and Peinado-Onsurbe, J. (2009) Lipoprotein lipase but not hormone-sensitive lipase activities achieve normality after surgically induced weight loss in morbidly obese patients. *Obes. Surg. 19*, 1150−1158.
(38) Jiang, Z. G., Robson, S. C., and Yao, Z. (2013) Lipoprotein metabolism in nonalcoholic fatty liver disease. *J. Biomed. Res. 27*, 1−13.
(39) Choi, S. H., and Ginsberg, H. N. (2011) Increased very low density lipoprotein (VLDL) secretion, hepatic steatosis, and insulin resistance. *Trends Endocrinol. Metab. 22*, 353−363.
(40) Li, X., Kypreos, K., Zanni, E. E., and Zannis, V. (2003) Domains of apoE required for binding to apoE receptor 2 and to phospholipids: Implications for the functions of apoE in the brain. *Biochemistry 42*, 10406−10417.
(41) Altmann, S. W., Davis, H. R., Jr., Yao, X., Laverty, M., Compton, D. S., Zhu, L. J., Crona, J. H., Caplen, M. A., Hoos, L. M., Tetzloff, G., Priestley, T., Burnett, D. A., Strader, C. D., and Graziano, M. P. (2002) The identification of intestinal scavenger receptor class B, type I (SR-BI) by expression cloning and its role in cholesterol absorption. *Biochim. Biophys. Acta, Mol. Cell Biol. Lipids 1580*, 77−93.
(42) Rigotti, A., Trigatti, B. L., Penman, M., Rayburn, H., Herz, J., and Krieger, M. (1997) A targeted mutation in the murine gene encoding the high density lipoprotein (HDL) receptor scavenger receptor class B type I reveals its key role in HDL metabolism. *Proc. Natl. Acad. Sci. U. S. A. 94*, 12610−12615.
(43) Mahley, R. W., and Huang, Y. (1999) Apolipoprotein E: from atherosclerosis to Alzheimer's disease and beyond. *Curr. Opin. Lipidol. 10*, 207−217.
(44) Kuipers, F., Jong, M. C., Lin, Y., Eck, M., Havinga, R., Bloks, V., Verkade, H. J., Hofker, M. H., Moshage, H., Berkel, T. J., Vonk, R. J., and Havekes, L. M. (1997) Impaired secretion of very low density lipoprotein-triglycerides by apolipoprotein E- deficient mouse hepatocytes. *J. Clin. Invest. 100*, 2915−2922.
(45) Huang, Y., Liu, X. Q., Rall, S. C., Jr., Taylor, J. M., von Eckardstein, A., Assmann, G., and Mahley, R. W. (1998) Over-expression and accumulation of apolipoprotein E as a cause of hypertriglyceridemia. *J. Biol. Chem. 273*, 26388−26393.
(46) Tsukamoto, K., Maugeais, C., Glick, J. M., and Rader, D. J. (2000) Markedly increased secretion of VLDL triglycerides induced by gene transfer of apolipoprotein E isoforms in apoE-deficient mice. *J. Lipid Res. 41*, 253−259.
(47) Seo, T., Al-Haideri, M., Treskova, E., Worgall, T. S., Kako, Y., Goldberg, I. J., and Deckelbaum, R. J. (2000) Lipoprotein lipase-mediated selective uptake from low density lipoprotein requires cell surface proteoglycans and is independent of scavenger receptor class B type 1. *J. Biol. Chem. 275*, 30355−30362.
(48) Hu, L., van der Hoogt, C. C., Espirito Santo, S. M., Out, R., Kypreos, K. E., van Vlijmen, B. J., van Berkel, T. J., Romijn, J. A., Havekes, L. M., Van Dijk, K. W., and Rensen, P. C. (2008) The hepatic uptake of VLDL in lrp-ldlr−/−vldlr−/− mice is regulated by LPL activity and involves proteoglycans and SR-BI. *J. Lipid Res. 49*, 1553−1561.
(49) Martineau, C., Kevorkova, O., Brissette, L., and Moreau, R. (2014) Scavenger receptor class B, type I (Scarb1) deficiency promotes osteoblastogenesis but stunts terminal osteocyte differentiation. *Physiol. Rep. 2*, e12117.
(50) Martineau, C., Martin-Falstrault, L., Brissette, L., and Moreau, R. (2014) The atherogenic Scarb1 null mouse model shows a high bone mass phenotype. *Am. J. Physiol Endocrinol. Metab 306*, E48−E57.
(51) Moller, C. L., Raun, K., Jacobsen, M. L., Pedersen, T. A., Holst, B., Conde-Frieboes, K. W., and Wulff, B. S. (2011) Characterization of murine melanocortin receptors mediating adipocyte lipolysis and examination of signalling pathways involved. *Mol. Cell. Endocrinol. 341*, 9−17.
(52) Karavia, E. A., Zvintzou, E., Petropoulou, P. I., Xepapadaki, E., Constantinou, C., and Kypreos, K. E. (2014) HDL quality and functionality: what can proteins and genes predict? *Expert Rev. Cardiovasc. Ther. 12*, 521−532.
(53) Marcel, Y. L., Weech, P. K., Nguyen, T. D., Milne, R. W., and McConathy, W. J. (1984) Apolipoproteins as the basis for heterogeneity in high-density lipoprotein2 and high-density lipoprotein3. Studies by isoelectric focusing on agarose films. *Eur. J. Biochem. 143*, 467−476.
(54) Tsompanidi, E. M., Brinkmeier, M. S., Fotiadou, E. H., Giakoumi, S. M., and Kypreos, K. E. (2009) HDL biogenesis and functions: Role of HDL quality and quantity in atherosclerosis. *Atherosclerosis 208*, 3−9.
(55) Kypreos, K. E., Gkizas, S., Rallidis, L. S., and Karagiannides, I. (2013) HDL particle functionality as a primary pharmacological target for HDL-based therapies. *Biochem. Pharmacol. 85*, 1575−1578.

DOI: 10.1021/acs.biochem.5b00700
Biochemistry 2015, 54, 5605−5616